Atmos. Chem. Phys. Discuss., 8, 20283–20309, 2008
www.atmos-chem-phys-discuss.net/8/20283/2008/

Atmospheric Chemistry and Physics Discussions

This discussion paper is/has been under review for the journal *Atmospheric Chemistry and Physics (ACP)*. Please refer to the corresponding final paper in *ACP* if available.

Assessing the regional impacts of Mexico City emissions on air quality and chemistry

M. Mena-Carrasco[1,2], G. R. Carmichael[3], J. E. Campbell[4], D. Zimmerman[5], Y. Tang[3], B. Adhikary[3], A. D'allura[6], L. T. Molina[2,7], M. Zavala[2,7], A. García[8], F. Flocke[9], T. Campos[9], A. J. Weinheimer[9], R. Shetter[9], E. Apel[9], D. D. Montzka[9], D. J. Knapp[9], and W. Zheng[9]

[1]Universidad Andrés Bello, Department of Environmental Engineering, Santiago, Chile
[2]Massachusetts Institute of Technology, Department of Earth, Atmospheric and Planetary Sciences, Cambridge, MA, USA
[3]The University of Iowa, Center for Global and Regional Environmental Research, Iowa City, IA, USA
[4]University of California at Merced, School of Engineering, Merced, CA, USA
[5]The University of Iowa, Department of Statistical and Actuarial Science, Iowa City, IA, USA

[6]Arianet Environmental Modeling, Milan, Italy
[7]Molina Center for Energy and the Environment, La Jolla, CA, USA
[8]Universidad Nacional Autónoma de México, Delegación Coyoacán, Mexico
[9]National Center for Atmospheric Research, Boulder, CO, USA

Received: 8 October 2008 – Accepted: 8 October 2008 – Published: 4 December 2008

Correspondence to: M. Mena-Carrasco (mmena@unab.cl)

Published by Copernicus Publications on behalf of the European Geosciences Union.

Abstract

The impact of Mexico City (MCMA) emissions is examined by studying its effects on air quality, photochemistry, and on ozone production regimes by combining model products and aircraft observations from the MILAGRO experiment. The influence of MCMA emissions to enhancements in surface level NO_x, CO, and O_3 concentrations are confined to distances <200 km. However, the extent of the influence is significantly larger at higher altitudes. Broader MCMA impacts (some 900 km Northeast of the city) are shown for specific outflow conditions in which enhanced ozone, NO_y, and MTBE mixing ratios over the Gulf of Mexico are linked to MCMA by source tagged tracers and sensitivity runs. This study shows that the "footprint" of MCMA on average is fairly local, with exception to reactive nitrogen, which can be transported long range in the form of PAN, acting as a reservoir and source of NO_x with important regional ozone formation implications. The simulated effect of MCMA emissions of anthropogenic aerosol on photochemistry showed a maximum regional decrease of 40% in $J[NO_2 \rightarrow NO+O]$, and resulting in the reduction of ozone production by 5–10%. Observed ozone production efficiencies and photolysis rates are evaluated as a function of distance from MCMA, and by modeled influence from MCMA. These tend to be much lower closer to MCMA, and with higher MCMA influence. This research shows that MCMA emissions have a discernible effect on regional air quality and photochemistry, both contributing large amounts of ozone and its precursors, but with caveat that aerosol concentrations hinder formation of ozone to its potential due to its reduction in photolysis rates.

1 Introduction

Megacities are defined as metropolitan areas with more than 10 million people (Gurjar and Lelieveld, 2005). This high concentration of urban dwellers generates challenging conditions for government: traffic congestion, solid and liquid waste disposal, drinking water supply, and bad air quality (Mayer, 1999; Lynn, 1999). Projections suggest that

ACPD

8, 20283–20309, 2008

these problems will worsen as more people are migrating from rural to urban areas (Saier, 2008), especially in the developing world, where most new megacities are located. In addition to the adverse impacts on ecosystems and human health at local scales, megacities may also have noticeable impacts on regional air quality and photochemistry (Mage et al., 1996; Guttikunda et al., 2003, 2005; Madronich, 2006; Gurjar and Lelieveld, 2005).

Mexico City Metropolitan Area (MCMA), with a population of 20 million, is located at 2200 m above sea level and has complex constraining topography. Its physical properties generate conditions for low combustion efficiency and entrainment of pollutants. Additionally traffic congestion, a relatively old vehicular fleet, and the concentration of economic and industrial activity make it one of the most polluted cities in the world (Molina, 2002, 2007). Megacities such as MCMA are also the source of considerable amounts of particulates, which affect photochemical reactions involved in ozone production and destruction (Carslaw and Carslaw, 2001) mainly by altering the amount of radiation involved in photochemical reactions. For example a study in the MCMA showed that observed photolysis rates of NO_2 at an urban site were 10–30% lower than at a nearby rural site (Raga et al., 2001). Model sensitivity studies in Asia and North America have shown that regional photochemistry can be altered by as much as 20% in the presence of aerosol (Tang, 2003; Li, 2005).

An intensive atmospheric chemistry measurement campaign denominated MILAGRO (Megacity Initiative: Local and Global Research Observations) (Fast et al., 2007; Molina et al., 2008) was carried out during March 2006, collecting chemical and meteorological data in the MCMA and surrounding areas. Besides the use of ground-based measurement platforms, the campaign included multiple aircrafts: DC-8, and J-31 supported by NASA, C-130 supported by NCAR-NSF, G-1 and B200 supported by DOE, and a Twin Otter supported by the US Forest Service and NSF. This paper focuses on the analysis of observations from the C-130 and DC-8. The spatial coverage, maneuverability and sampling strategies for these aircrafts were different. The C-130 sampled near and within the city, performing zig-zags and spirals at multiple altitudes with an

ACPD
8, 20283–20309, 2008

altitude range from 0–6.5 km above mean sea level (MSL), with most measurements being taken in Mexico City or the Gulf of Mexico. The DC-8 performed direct flights from Houston, TX, with limited spirals, and a higher altitude range (0–12 km above MSL). With the different spatial coverage, these aircraft sampling strategies intended to evaluate the regional influence of MCMA emissions on a regional (C-130), and continental (DC-8) scale.

In this paper we examine the impact of MCMA's emissions on ozone production focusing on interactions between ozone precursor concentrations and photochemistry. Using a combination of observations and model sensitivity analyses we estimate MCMA's "air quality" footprint. The area required to provide water, food, energy and waste management services to a megacity has been defined as the ecological footprint, which has been estimated to be significantly larger than the city itself (Valentine and Heiken, 2000). Here we extend such analysis to look at the "air quality footprint" of the MCMA emissions, which we define as the geographical extension of discernible enhancements (contributions) of concentrations and photochemical rates attributable to the MCMA.

2 Methods

2.1 Model description

2.1.1 Meteorological and chemical transport model

In this campaign we used the STEM-2K3 model (Carmichael et al., 2003) to carry out air quality forecasting simulations to provide support and context to aircraft observations during the campaign. This chemical transport model (CTM) features full chemistry calculations using a lumped species SAPRC99 chemical mechanism (Carter, 2000) in conjunction with the TUV (Tropospheric Ultraviolet Radiation Model) (Madronich et al., 1992) on-line photolysis model and the SCAPE II (Simulating Composition of Atmo-

ACPD
8, 20283–20309, 2008

spheric Particles in Equilibrium aerosol solver (Kim et al., 1993, 1995, 2003). The calculation of the photolysis was two-way coupled with other chemical modules, including inputs of concentrations of aerosols and gas phase species, and outputs of 30 photolysis rates defined by the SAPRC99 mechanism. The STEM-2K3 model was driven by the WRF V2.1.2 (Weather Research Forecasting) meteorological model (Grell et al., 2005), using the NCEP (National Center for Environmental Prediction) Global Forecasting System (GFS) 1°×1° analyses for meteorological boundary conditions (NCEP, 2003). For this study the model simulations used two nested domains, the outer using a 60 km resolution, 100 cells in East-West direction, and 64 cells in North-South direction, with an inner domain using a 12 km resolution, 110 cells East-West, and 95 cells North-South. The model had 21 vertical layers, extending from the surface to 100 hPa, with 10 of the levels representing altitudes from surface to 1 km above the terrain. The Grell Grell-Devenyi ensemble cumulus parameterization (Grell et al., 1995), the YSU planetary boundary layer parameterization (Hong et al., 2006), and the Noah land surface model (NOAA, 2005) were used for the WRF runs. In addition, tagged non-reactive tracer calculations were performed to qualitatively assess the contribution of geographical areas and source categories (MCMA, Northern Mexico, Southern Mexico, Central America, Texas, Central America, Asia, South East United States, biomass burning, large point sources, total anthropogenic CO, biogenic CO) to CO mixing ratios.

The simulation period was March 2006, including a one week model spin-up.

2.1.2 Emissions inventories and boundary conditions

The model runs used a high resolution emissions inventory for the MCMA developed by Universidad Nacional Autónoma de México (UNAM) for 1999 (Tie et al., 2007), which included speciated VOC which were lumped into the SAPRC99 VOC categories. For surrounding areas of MC, south of 21° N the Emission Database for Global Atmospheric Research (EDGAR 2.0) 1° resolution anthropogenic area emissions inventory for 1990 was used (Olivier et al., 2002). For the six states in Mexico that share a border with the US (Baja California, Sonora, Chihuahua, Coahuila, Nuevo León, and Tamauli-

ACPD
8, 20283–20309, 2008

pas) a 36 km resolution anthropogenic emissions inventory from the BRAVO (Big Bend Regional Aerosol and Visibility Observational) study (Kuhns et al., 2005) was used. Biomass burning emissions of CO were provided by the an ecosystem based wild fire emissions processor (Pierce et al., 2007) which is part of the RAQMS (Regional Air Quality Modeling System) model (Pierce et al., 2005). Biogenic emissions were estimated using BEIS 2 (Biogenic Emissions Inventory System) (Geron et al., 1994) that generates time-variable isoprene and monoterpene emissions driven by meteorological variables, in this case from WRF simulations

Chemical boundary conditions were obtained from the Model for Ozone and Related Chemical Tracers (MOZART) (Horowitz et al., 2003), which was run by NCAR at a 0.7° resolution using MOPITT assimilated CO concentrations for the same modeling period (March 2006) (Pfister et al., 2005).

2.2 Interpolation of observations

Aircraft measurements provide a unique opportunity to collect three dimensional observations of multiple chemical and meteorological parameters. Plotting these observations along flight tracks allow us to infer outflow patterns from the cities. However, interpolating these observations horizontally highlight these patterns even more. In this study we interpolated aircraft observations using kriging (Krige, 1951) for the nearest 50 observations and an isotropic exponential semi-variogram. Interpolations were performed using ArcView 9.2 Geostatistical Analyst. This method, which has been used before in interpolating point bias estimations for aircraft observations during INTEX-NA (Mena-Carrasco et al., 2007), is only valid if the uncertainty of the method (subject to the sampling strategy, and the data) is significantly lower than the range of the interpolated values, which was the case for the analysis presented below.

ACPD
8, 20283–20309, 2008

3 Results and discussion

The regional impacts of MCMA are analyzed in two different categories: impact on air quality levels (again, focusing on O_3, NO_2, and CO) and impact on photochemistry. While interrelated, these impacts are analyzed separately to estimate various aspects of the air quality "footprint" of MCMA emissions, which we define as the geographical extension of discernible enhancements (contributions) on concentrations of pollutants, or on photochemical rates. Before any conclusions or results can be presented, it is necessary to establish that the model performance is adequate. Table 1 shows a summary of some species correlation coefficients for ozone and some of its precursors support the conclusions drawn from this study. The base model run used in this study was the result of systematic improvement of model performance after the forecast stage of the campaign, focusing on updating boundary conditions from global models and analyzing model bias associated to emissions inventory errors (and how ozone precursor errors were correlated to ozone errors). In general the model does a good job in predicting the ambient levels of the trace gases (correlation coefficients of ~0.6 for all science flights), and in capturing the variability (i.e., the predicted and observed variability are very similar as measured by the ratio of the standard deviation devided by the mean values). Further details on the model performance can be found in a separate paper that focuses on model performance during the forecast stage, and improvements made by updating emissions inventories and boundary conditions (Mena-Carrasco et al., 2008).

3.1 Modeled contribution of MCMA to pollutants

There are many ways to estimate the impact of the emissions from the MCMA. The effects of MCMA on the regional distributions of pollutants calculated as the difference between mixing ratios of modeled species with and without MCMA emissions, normalized to mixing ratios without MCMC emissions are presented in Fig. 1. Shown are the mean daytime contribution of MCMA to near surface mixing ratios of NO_2, CO, and O_3

ACPD
8, 20283–20309, 2008

for 1–31 March 2006. These results indicate that the impact varies by species, with the largest effects found for the primary pollutants. For example, locally (less than 100 km from the Distrito Federal) the near surface contribution of MCMA to the primary pollutants CO and NO_2 is greater than 50%. Significant contributions from MCMA emissions on near surface levels of NO_2 and CO (20–50% for NO_2 and 10–20% for CO) can extend ~200 km north, based on model results. In the lower-mid troposphere (3 km layer, shown in bottom panels) smaller contributions of MCMA emissions to CO and NO_2 (5–10% and 10–20% contribution, respectively) can extend up to ~300 km north and south of the city, with those contributions to NO_2 reaching Tampico). The MCMA contribution is highest for the short lived species (e.g., NO_2), but it is also more geographically confined. In contrast, for longer-lived species (e.g., CO), the background levels are higher, and the contributions from the MCMA are smaller, but are spread over greater distances. The MCMA contribution to ozone levels is qualitatively similar to those for CO, and smaller than those for NO_2. The magnitude and structure of the ozone response reflects non-linearities in the ozone chemistry.

A day to day analysis shows that these patterns present great variability in terms of the extension and the intensity of the contribution of Mexico City emissions on surrounding areas (focusing on % contribution to NO_y, which in a way serve as a tracer for NO_x emissions). Comparing near surface contributions (Fig. 2) to mid troposphere contributions (Fig. 3) the MCMA influence is largest and most widespread at 3 km (with most of NO_y in the form of PAN, not shown). Modeled contributions from 20 to 50% in this layer are shown to extend well outside the boundaries of the country, both into the Pacific Ocean and the Gulf of Mexico. The MCMA regions of influence vary day-by-day in terms of rather distinct plumes (e.g., Fig. 3, 12 and 19 March) to more dispersed features (e.g., 14 March). Further discussions of the MCMA plumes are presented below.

ACPD
8, 20283–20309, 2008

3.2 18–19 March 2006 long range transport event

Specific synoptic features, such as a prevailing high pressure system over the Gulf of Mexico, and a low pressure system over Northwestern Mexico can favor transport events that can extend the region of influence of MCMA emissions on a regional scale, i.e., the 18–19 March 2006 period in which persistent westerly and southwesterly winds created favorable conditions for distinct long range transport (Fast et al., 2007). An important question that MILAGRO set out to answer was over what geographic scales can the effects of the MCMA plume be identified? In this section we explore various methods to establish the spatial extent of the plume using observations and modeling products, focusing on 19 March 2006. On this day the C-130 flew to intercept fresh emissions near the source, and then out into the Gulf of Mexico to intercept aged MCMA emissions (from previous days).

3.2.1 Interpolation of observations along flight track to illustrate outflow plume

Kriging was used to highlight the outflow pattern during the event, using O_3, NO_y, and methyl tertiary-butyl ether (MTBE) observations, the latter is a gasoline oxygenate linked to mobile source emissions that has a half life of 3 to 6 days (Achte, 2002). The results are shown in the top panels of Fig. 4. Shading in the figures represents the uncertainty of the interpolation method, which depends on the geographical distribution of the data. In this case uncertainty is substantially lower than the observations in the plume (15 ppb, 1.5 ppb, 5 ppt for O_3, NO_y and MTBE respectively). This method works under the assumption that the sampling captures largely the horizontal geospatial variations of the chemical species and that over the duration of the observations that the geospatial distributions are constant in time. These conditions are satisfied as the sampling strategy for this flight was to look specifically at the MCMA plume, and the sampling horizontal velocity of the aircraft is roughly 20 times faster (mean value of 125±0.47 m/s for a 95% confidence interval) than the transportation of pollutants (mean wind velocity of 6.79±0.15 m/s for a 95% confidence interval). The top pan-

ACPD
8, 20283–20309, 2008

els show plumes of O_3, NO_y and MTBE near MCMA and also off the coast of Texas. On this day the MCMA plume was being transported towards the north-northeast, and the C130 followed the plume to the coast. The flight continued out over the Gulf of Mexico and sampled the aged MCMA plume. The plume like structure is identified in the krieged fields and is similar to that predicted by the MCMA footprints, which are also shown in Fig. 4 (lower panels). These results suggest that the observation of the MCMA plume can be observed out to 900 KM. The center right panel shows the ratio of observed NO_x to NO_y. This ratio is high in MCMA reflecting fresh emissions. The value decreases with distance from the megacity, as the plume photochemical ages. When the aircraft encountered MCMA plumes transported over the Gulf on the previous day the ratio increased. In these older NO_y is mostly in the form of PAN, suggesting that the thermal decomposition of PAN may be an important source of NO_x, which contributes to additional ozone formation along the outflow, in agreement with work by Emmons et al. (2008).

3.2.2 Time series of modeled and observed values along flight track

Through the combination of the measurements and models it is possible to develop strategies to identify individual observations that are impacted by the MCMA. For example the model predictions of MCMA impact can be sampled along the flight paths, merged with the observational data, and then used as a filter to collect data that meet specified design criteria. An example is shown in Fig. 5, where observed and predicted O_3 and NO_y mixing ratios are plotted along the flight path for the 19 March flight discussed above. Each predicted data point is colored by the % contribution of the MCMA tracer to CO. The predicted values of O_3 and NO_y agree reasonably well (R=0.72 for O_3 and 0.76 for NO_y) with the observations and capture much of the observed structure and variability. The results indicate the contributions of the MCMA vary significantly along the flight path. Near the MCMA local emissions dominate as shown by the high MCMA contributions at 12:00–13:00 and 18:00–19:00 local time (LT). As as discussed above and shown in Fig. 4, during this flight elevated levels of ozone and NOy (60

ACPD
8, 20283–20309, 2008

and ~2 ppbv, respectively) were observed off the coast of Texas. This sampling period corresponds to period 15:00–16:00 LT in Fig. 5. For these points the emissions from the MCMA show a ~50–60% modeled contribution to CO. Application of this screening approach are presented in the following section.

3.2.3 Impact of MCMA emissions on ozone formation and regional photochemistry

To evaluate the effect of MCMA on ozone formation we focus on calculating ozone production efficiency (OPE) (Kleinman, 2002), defined as the amount of odd oxygen vs. NO_x lost (sum of odd oxygen NO_2+O_3 vs. NO_z). Observed ozone production efficiencies for all the C-130 flights are shown in Fig. 6. The data are identified by distance from MCMA (left panel) and by contribution from MCMA emissions (right panel). Near the city, ozone production efficiencies are lower than at further from the city (4.9 vs. 7.9 respectively). Similarly, categorizing observations with large MCMA influences (using over 30% modeled contribution to NO_y as the metric for significant MCMA contribution) we see that OPE is lower than those with smaller MCMA influences (5.3 vs. 6.9 respectively). These effects are expected as high NO_x mixing ratios, tend to form nitric acid (HNO_3, a component of NO_z) under a VOC limited ozone production regime (Tie, 2007), making ozone production less efficient. Also, while Mexico City shows VOC limited conditions, it does still present large VOC concentrations (Karl et al., 2008) and as it ages forms PAN, which hinders O_3 formation locally, but downwind contributes to formation as a remote source of NO_x (Emmons et al., 2008).

Another important consideration in regards to ozone production and photochemical activity is the role of aerosols. Mexico City is a large source of absorbing and scattering aerosol (Marley et al., 2007). The aerosols impact the photochemistry in various ways. One important impact is that the aerosol change the photolysis rates. In order to evaluate the effect of MCMA aerosol on photochemistry and ozone formation, sensitivity runs were performed analyzing the difference between a full chemistry run and a run in which the effect of aerosol on the online calculated photolysis rates is excluded (No-AOD run). For this case we focused on the 10 March 2006 outflow event.

ACPD
8, 20283–20309, 2008

The general features for this day are shown in Figs. 2 and 3. It was found that for $J[NO_2]$ (the most direct photochemical ozone formation reaction), aerosols were found to reduce the photolysis rates by up to 40% in areas downwind of MCMA to the NE, and reduce ozone mixing ratios by as much as ~5–10%. This amounts to changes in ozone levels between 5 to 10 ppb. The large regional extent of the effect of aerosols on the photochemistry is due to the fact that in megacities aerosol and ozone precursors are co-emitted and are transported together, leading to a prolonged influence on photochemistry (Tang, 2003).

However these impacts may indeed be underestimated, if we look at how the model captures the effect of aerosols on photolysis. If we try to show the spatial distribution of point bias calculations interpolated for all flights (Fig. 8) we see that photolysis rates are overpredicted between 10 to 50% especially near MCMA. These results suggest that the modeled effect of aerosol on photochemistry is most likely a conservative estimation. A major cause of the underestimation of the impact of aerosols may be due to the underprediction in emissions in wind blown dust and biomass burning, which are represented in the model with a high degree of uncertainty. Both dust and biomass burning aerosols were observed at high levels during this time period in and around the city. Thus high aerosol concentrations clearly contribute to low ozone production efficiency near the MCMA due to the reduction in photolysis rates, which tends to keep NO_x levels elevated in the city. The low photolysis rates also increase the lifetime of NO_2, thus pushing peak ozone production farther downwind.

4 Conclusions

These results show that the MCMA emissions have a discernible impact in regional air quality and photochemistry. MCMA emissions contribute to the majority of local mixing ratios of CO and NO_2, but contributions of 10–30% in near surface CO and NO_y can extend up to 200 kilometers. Broader geographical MCMA impacts (some 900 km Northeast of the city) are shown for specific outflow conditions (19 March 2006 C-130

ACPD
8, 20283–20309, 2008

flight) in which enhanced ozone, NO_y, and MTBE mixing ratios over the Gulf of Mexico are linked to MCMA by tagged tracers using a chemical transport model. The effect of aerosols on photochemistry and ozone formation can be large; e.g., photolysis rates of NO_2 can be reduced regionally by up to 40%, while ozone formation can be reduced by 5–10% near the surface. In addition, observed ozone production efficiency is lower near MCMA (<100 km) than surrounding areas. Similarly airmasses under large MCMA influence also show lower ozone production efficiency than those with smaller MCMA influence. This research shows that MCMA emissions impact the regional environment in important ways with broad influences on air quality, photochemistry, and ozone production. However, these influences vary significantly with synoptic conditions. These influences become more subtle with distance. Thus the establishment of the air pollution footprint of megacities in general, and MCMA specifically, is a challenging problem, and one that cannot be determined by observations themselves. Here we show that the use of novel interpolation of aircraft observations through kriging, in conjunction with model products, can provide geographical context and qualitative categorization of the influence of MCMA emissions. This research shows that while MCMA emissions have a discernible effect on regional air quality and photochemistry, both contributing large amounts of ozone and its precursors, aerosol concentrations hinder formation of ozone to its potential due to its reduction in regional photolysis rates.

Acknowledgements. This work was funded in part by research grants by NASA and NSF (ATM Award 0528227 to MIT). Special thanks to the MILAGRO science team for providing high quality chemical observations in a timely fashion. Special thanks to Jerome Fast, Brad Pierce, Larry Kleinman, Louisa Emmons, and Sasha Madronich.

References

Achte, C., Puttman, W., and Klasmeir, J.: Compartment modeling of mtbe in the generic environment and estimations of the aquatic mtbe input in germany using the eqc model, J. Environ. Monitor., 4, 747–752, doi:710.1039/b201879a, 2002.

Carmichael, G. R, Tang, Y., Kurata, G., Uno, I., Streets, D., Woo, J. H., Huang, H., Yienger, J., Lefer, B., Shetter, R., Blake, D., Atlas, E., Fried, A., Apel, E., Eisele, F., Cantrell, C., Avery, M., Barrick, J., Sachse, G., Brune, W., Sandholm, S., Kondo, Y., Singh, H., Talbot, R., Bandy, A., Thorton, D., Clarke, A., Heikes, B.: Regional-scale chemical transport modeling in support of the analysis of observations obtained during the trace-p experiment, J. Geophys. Res.-Atmos., D21, 8823, doi:10.1029/2002JD003117, 2003.

Carslaw, N. and Carslaw, D.: The gas-phase chemistry of urban atmospheres, Surv. Geophys., 22, 31–53, 2001.

Carter, W. P. L.: Documentation of the saprc-99 chemical mechanism for voc reactivity assessment, final report to california air resources board, Contract No. 92-329, University of California, Riverside, 8 May, 2000.

Emmons, L., Pfister, G., Madronich, S., et al.: Impact of mexico city emissions on regional air quality from mozart-4 simulations, in preparation, 2008.

Fast, J. D., de Foy, B., Acevedo Rosas, F., Caetano, E., Carmichael, G., Emmons, L., McKenna, D., Mena, M., Skamarock, W., Tie, X., Coulter, R. L., Barnard, J. C., Wiedinmyer, C., and Madronich, S.: A meteorological overview of the MILAGRO field campaigns, Atmos. Chem. Phys., 7, 2233–2257, 2007, http://www.atmos-chem-phys.net/7/2233/2007/.

Geron, C., Guenther, A., and Pierce, T.: An improved model for estimating emissions of volatile organic compounds from forests in the eastern united states, J. Geophys. Res.-Atmos., D6, 12 773–12 792 doi:12710.11029/12794JD00246, 1994.

Grell, G., Dubhia, J., and Stauffer, D. R.: Description of the fifth generation penn state/ncar mesoscale model (mm5), http://cng.ateneo.net/cng/wyu/resources/mm5/desc/cover.pdf, accessed June 2006, 1995.

Grell, G. A., Peckham, S. E., Schmitz, R., McKeen, S. A., Frost, G., Skamarock, W. C., and Eder, B.: Fully coupled "Online" Chemistry within the wrf model, Atmos. Environ., 39, 6957–6975, 2005.

Gurjar, B. R. and Lelieveld, J.: New directions: Megacities and global change, Atmos. Environ., 39, 391, 2005.

Gurjar, B. R., Butler, T. M., Lawrence, M. G., and Lelieveld, J.: Evaluation of emissions and air quality in megacities, Atmos. Environ., 42, 1593–1606, 2008.

Guttikunda, L. Guttikunda, S. K., Tang, Y. H., Carmichael, G. R., Kurata, G., Pan, L., Streets, D. G., Woo, J. H., Thongboonchoo, N., and Fried, A.: Impacts of asian megacity emissions

on regional air quality during spring 2001, J. Geophys. Res.-Atmos., D20, 1–27, 2005.
Guttikunda, S. K., Carmichael, G. R., Calori, G., Eck, C., and Woo, J.-H.: The contribution of megacities to regional sulfur pollution in asia, Atmos. Environ., 37, 11, 11–22, 2003.
Hong, S.-Y., Noh, Y., and Dudhia, J.: A new vertical diffusion package with an explicit treatment of entrainment processes, Monthly Weather Review, 134, 2318–2341, 2006.
Horowitz, L. W., Walters, S., Mauzerall, D., et al: A global simulation of tropospheric ozone and related tracers: Description and evaluation of mozart, version 2, J. Geophys. Res.-Atmos., D24, 4784, doi:4710.1029/2002JD002853, 2003.
Kim, Y. P. and Seinfeld, J. H.: Atmospheric gas-aerosol equilibrium iii: Thermodynamics of crustal elements ca2+, k+, mg2+, Aerosol Sci. Technol., 22, 93–110, 1995.
Kim, Y. P., Seinfeld, J. H., and Saxena, P.: Atmospheric gas-aerosol equilibrium i: Thermodynamic model, Aerosol Sci. Technol., 19, 151–181, 1993.
Kim, Y. P., Seinfeld, J. H., and Saxena, P.: Atmospheric gas-aerosol equilibrium ii: Analysis of common approximations and activity coefficient calculation methods, Aerosol Sci. Technol., 19, 182–198, 2003.
Kleinman, L., Daum, P., Lee, Y., Nunnermacker, L., and Springton, S.: Ozone production efficiency in an urban area, J. Geophys. Res.-Atmos., 107, p. 4733, 2002.
Krige, D. G.: A statistical approach to some mine valuations and allied problems at the witwatersrand, Master's thesis of the University of Witwatersrand, 1951.
Kuhns, H. and Vukovich, K. E.: JM Development of a United States-Mexico emissions inventory for the big bend regional aerosol and vility observationsl (bravo) study, of the Air Waste Management Association, 55, 677, 677–692, 2005.
Li, G., Zhang, R., Fan, J., and Tie, X.: Impacts of black carbon aerosol on photolysis frequencies and ozone in the houston area, J. Geophys. Res.-Atmos., 110, D23206, doi:10.1029/2005JD005898, 2005.
Lynn, W.: Megacities: Sweet dreams or environmental nightmares?, Environ. Sci. Technol., 33, 238A–240A, 1999.
Madronich, S.: Implications of recent total atmospheric ozone measurements for biologically-active ultraviolet-radiation reaching the earths surface, Geophys. Res. Lett., 19, 37–40, 1992.
Madronich, S.: Chemical evolution of gaseous air pollutants down-wind of tropical megacities: Mexico city case study, Atmos. Environ., 40, 6012, doi:10.1016/j.atmosenv.2005.08.047, 2006.

Mage, D., Ozolins, G., Peterson, P., Webster, A., Orthofer, R., Vandeweerd, V., and Gwynne, M.: Urban air pollution in megacities of the world, Atmos. Environ., 30, 681, doi:10.1016/1352-2310(95)00219-7, 1996.

Marley, N. A., Gaffney, J. S., Ramos-Villegas, R., and Cárdenas González, B.: Comparison of measurements of peroxyacyl nitrates and primary carbonaceous aerosol concentrations in Mexico City determined in 1997 and 2003, Atmos. Chem. Phys., 7, 2277–2285, 2007, http://www.atmos-chem-phys.net/7/2277/2007/.

Mayer, H.: Air pollution in cities, Atmos. Environ., 33, 4029, doi:10.1016/S1352-2310(99)00144-2, 1999.

Mena-Carrasco, M., Tang, Y., Carmichael, G., et al.: Improving regional ozone modeling through systematic evaluation of errors using the aircraft observations during the international consortium for atmospheric research on transport and transformation, J. Geophys. Res.-Atmos., 112, D12S19, doi:10.1029/2006JD007762, 2007.

Mena, M., Carmichael, G. R., and Molina, L. T.: Improving regional emissions inventories using sistematic data analysis of model performance during milagro, in preparation, 2008.

Molina, L. T., Kolb, C. E., de Foy, B., Lamb, B. K., Brune, W. H., Jimenez, J. L., Ramos-Villegas, R., Sarmiento, J., Paramo-Figueroa, V. H., Cardenas, B., Gutierrez-Avedoy, V., and Molina, M. J.: Air quality in North America's most populous city - overview of the MCMA-2003 campaign, Atmos. Chem. Phys., 7, 2447–2473, 2007, http://www.atmos-chem-phys.net/7/2447/2007/.

Molina, L. T. and Molina, M.: Air quality in mexico megacity, an integrated assessment, published by Kluwer, 2002.

NCEP: The global forecasting system, NCEP Office Note 442, http://www.emc.ncep.noaa.gov/mmb/gcp/noahlsm/README_2.2.htm, 2003.

NOAA: The community noah land surface model, Users Guide Public Version 2.7.1, http://www.emc.ncep.noaa.gov/mmb/gcp/noahlsm/Noah_LSM_USERGUIDE_2.7.1.htm, 2005.

Olivier, J. G. J., Maas, B. A., van der, C. W. M., Berdowski, J. J. M., Veldt, C., Bloos, J. P. J., Visschedijk, A. J. H, Zandveld, P. Y. J., and Haverlag, J. L: Application of edgar. , RIVM report 73301001, 2267–2288, 2002.

Pfister, G., Hess, P. G., Emmons, L. K., Lamarque, J.-F., Wiedimeyer, C., Edwards, C. P., Petron, G., Gille, J. C., and Sachse, G. W.: Quantifying co emissions from the 2004 alaskan wilfires using mopitt-co data, Geophys. Res. Lett., 32, L11809, doi:11810.11029/12005GL022995, 2005.

Pierce, R. B., Olivier, J., Bouwman, A., van der Maas, C., Berdowski, J., Veldt, C., Bloos, J., Visschedijk, A., Zandveld, P., and Haverlag, J.: Regional air quality modeling system (raqms) predictions of the tropospheric ozone budget over east asia, J. Geophys. Res.-Atmos., D21, 8825, doi:10.1029/2002jd003176, 2003.

Pierce, R. B., Schaack, T., Al-Saadi, J. A., et al.: Chemical data assimilation estimates of continental US Ozone and nitrogen budgets during the intercontinental chemical transport experiment – north america, J. Geophys. Res.-Atmos., D21, doi:10.1029/2006JD007722 D12S21, 2007.

Raga, G. B., Castro, T., and Baumgardner, D.: The impact of megacity pollution on local climate and implications for the regional environment: Mexico city, Atmos. Environ., 35, 1805, doi:10.1016/S1352-2310(00)00275-2, 2001.

Saier, M. H.: Are megacities sustainable?, Water Air and Soil Pollution, 191, 1–3, 2008.

Tang, Y. H., Carmichael, G. R., Uno, I., et al.: Impacts of aerosols and clouds on photolysis frequencies and photochemistry during trace-p: 2. Three-dimensional study using a regional chemical transport model, J. Geophys. Res.-Atmos., D21, 8822, doi:10.1029/2002JD003100, 2003.

Tie, X., S. M., G. Li, Z. Ying, R., Zhang, A., Garcia, R., Lee-Taylor, J., and Liu, Y.: Characterizations of chemical oxidants in mexico city: A regional chemical dynamical model (wrf-chem), Atmos. Environ., 41, 1989–2008, 2007.

Valentine, G. A. and Heiken, G.: The need for a new look at cities, Environ. Sci. Policy, 3, 231–234, 2000.

ACPD

8, 20283–20309, 2008

Table 1. Model performance statistics for selected species during MILAGRO. C-130 Platform. 0–6 km range, flights 1–13.

	O_3 (n=4066)		CO (n=3213)		C_3H_8 (n=3936)		ARO_1 (n=1176)	
	Obs	Mod	Obs	Mod	Obs	Mod	Obs	Mod
Mean	58.73	66.12	146.86	184.72	1.84	1.98	0.27	0.34
SD/mean	0.33	0.29	0.58	0.46	1.77	1.84	2.00	2.68
R		0.58		0.67		0.75		0.64
MNB		0.10		0.25		0.07		0.26
	NO_x(n=4226)		NO(n=4259)		NO_2(n=4312)		NO_y(n=3936)	
	Obs	Mod	Obs	Mod	Obs	Mod	Obs	Mod
Mean	0.82	0.51	0.16	0.12	0.65	0.38	2.99	3.57
SD/mean	4.40	2.70	2.87	3.75	2.85	2.73	1.53	1.45
R		0.70		0.55		0.71		0.63
MNB		−0.38		2.1		−0.41		0.19

SD: standard deviation. MNB: Mean normalized bias, calculated as mean bias divided by mean average times 100. ARO_1: Based on SAPRC99 speciation, it is defined as the sum of benzene and toluene.

ACPD
8, 20283–20309, 2008

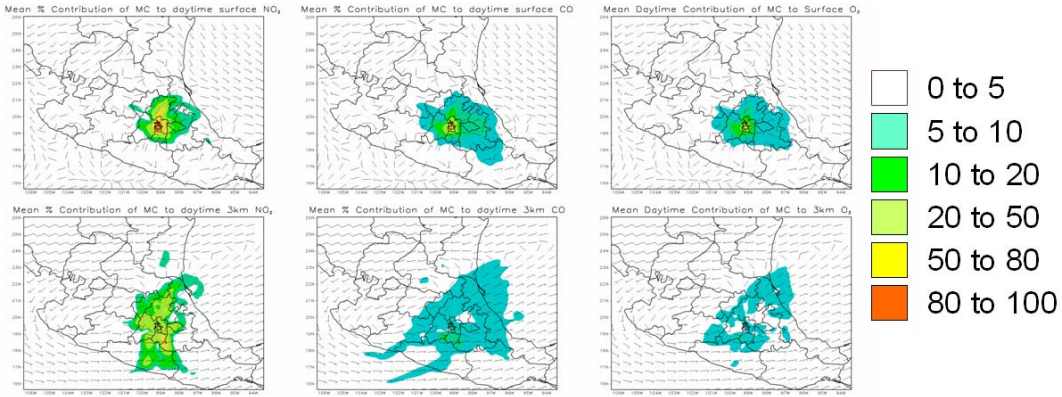

Fig. 1. Calculated effect of Mexico City on mean 18 Z mixing ratios for March 2006. Top left: Mean % contribution to near surface CO. Top center: NO_2. Top right: O_3. Bottom left: Mean % contribution to CO for 3 km above surface level. Top center: NO_2. Top right: O_3. Contribution calculated as difference between simulated values with and without Mexico City emissions.

ACPD
8, 20283–20309, 2008

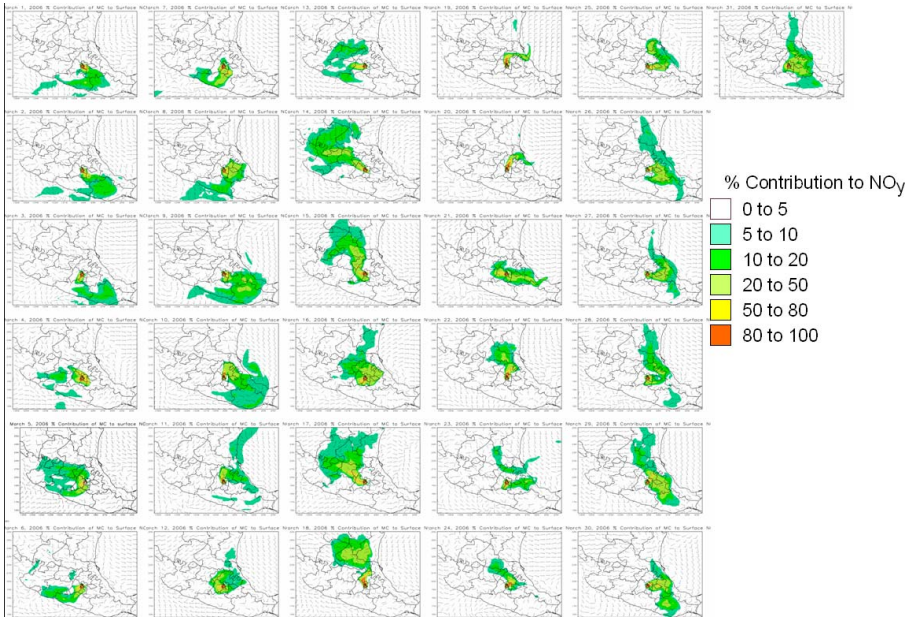

Fig. 2. Calculated effect of Mexico City emissions on 18 Z mixing ratios of NO_y for 1–31 March 2006, shown as the % contribution for the near surface layer. Contribution calculated as percent difference between simulated values with and without Mexico City emissions.

ACPD

8, 20283–20309, 2008

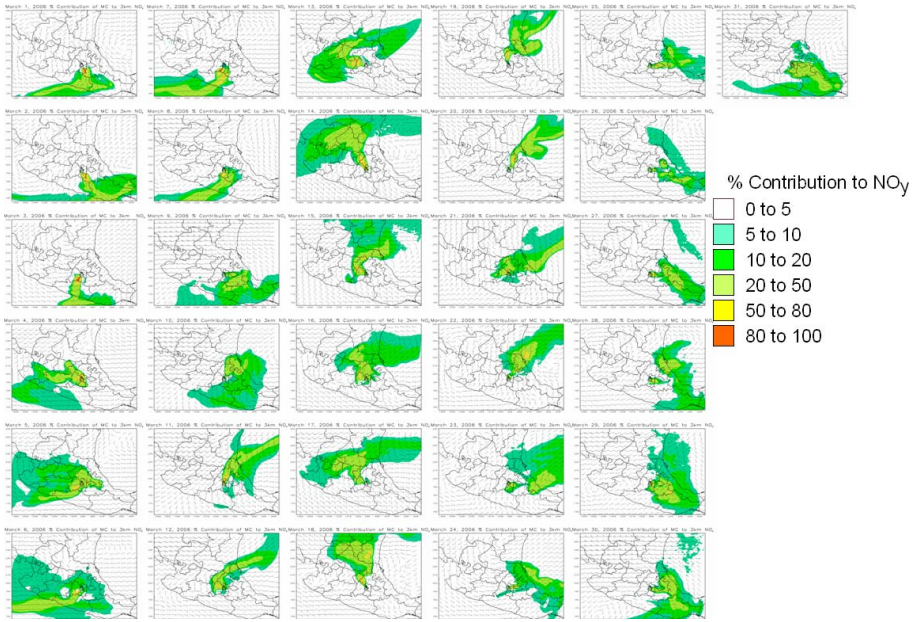

Fig. 3. Calculated effect of Mexico City emissions on 18 Z mixing ratios of NO_y for 1–31 March 2006, shown as the % contribution for the 3 km above surface vertical layer. Contribution calculated as percent difference between simulated values with and without Mexico City emissions.

ACPD

8, 20283–20309, 2008

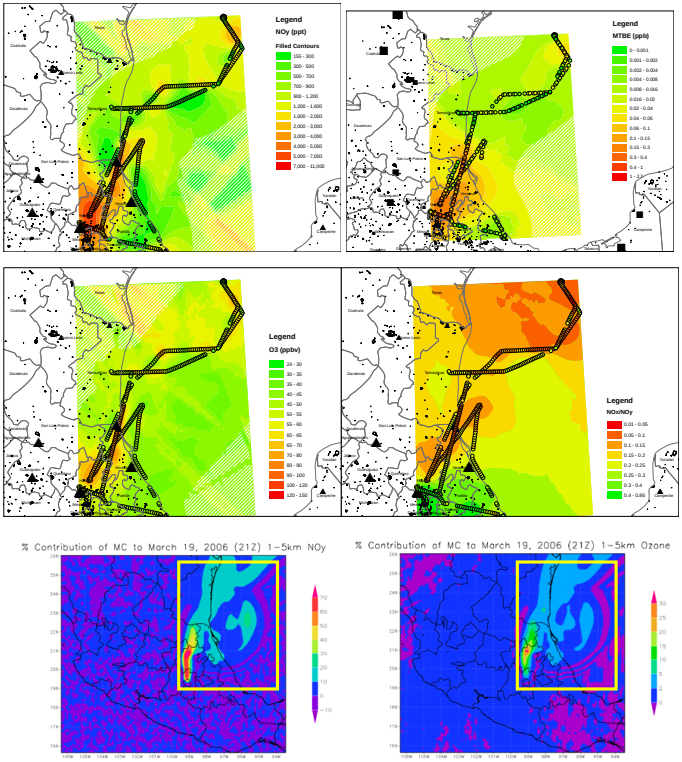

Fig. 4. Interpolated observations through kriging for C-130 19 March 2006 flight. Top Left: MTBE Right: NO_y. Center left: O_3, Center right: NO_x/NO_y, 5 Calculated effect of Mexico City on regional air quality. Shaded area represents method uncertainly for NO_y (1500 pptv), NO_x (800 pptv) and O_3 (15 ppbv) Bottom Left: Simulated contribution to mean 1–5.4 km NO_y. Bottom Right: Simulated percent contribution to 19 March 2006 (21 Z) 1–5.4 km mean ozone, calculated as the difference in mixing ratios with and without Mexico City anthropogenic emissions.

ACPD
8, 20283–20309, 2008

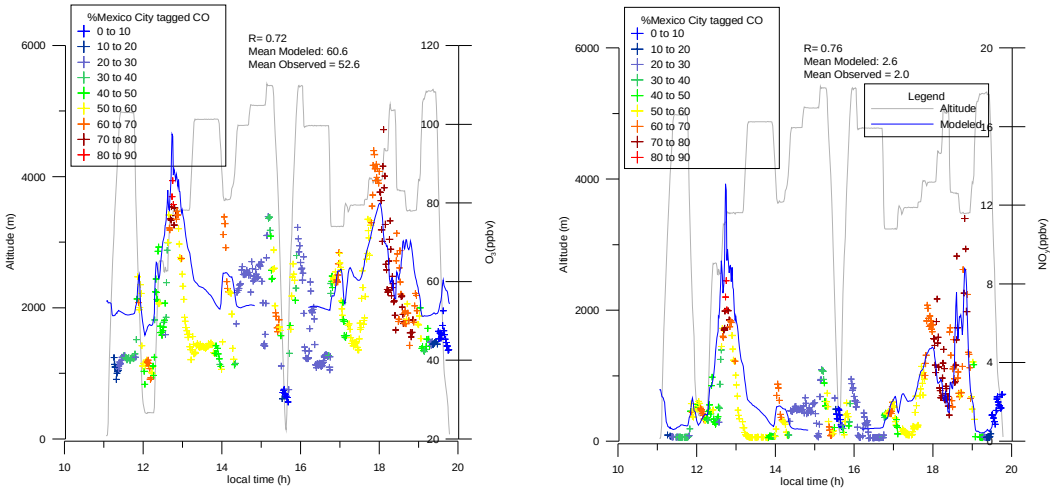

Fig. 5. Times series of observed and predicted O_3 and NO_y along 19 March 2006 C-130 flight track. Points are colored by the contribution of Mexico City tracer CO to total tracer CO. Left: O_3 (ppbv), Right: NO_y(ppbv)

ACPD
8, 20283–20309, 2008

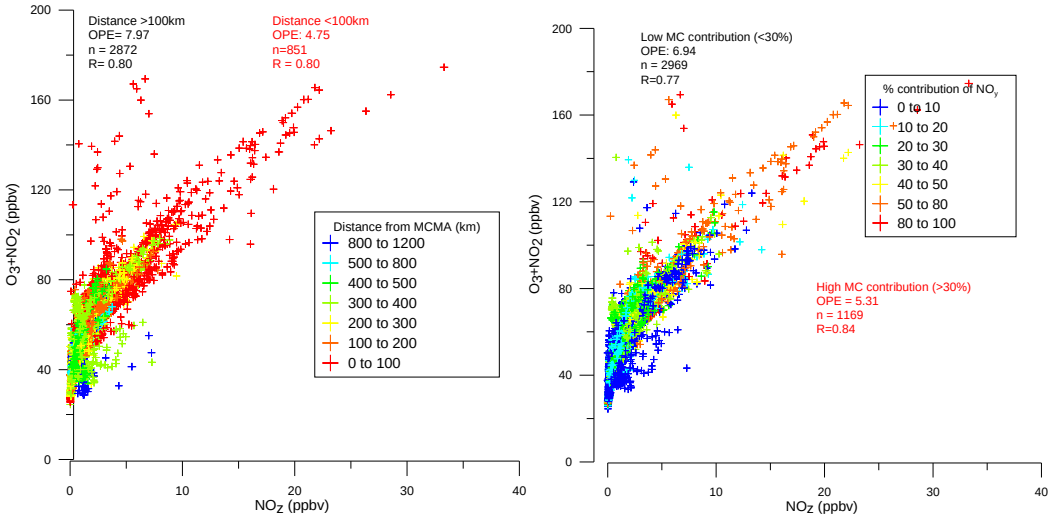

Fig. 6. Observed ozone production efficiencies, derived from O_3+NO_2 and NO_z observations as a function of distance (Left) and modeled influence of Mexico City emissions (Right) for all C-130 flights.

ACPD
8, 20283–20309, 2008

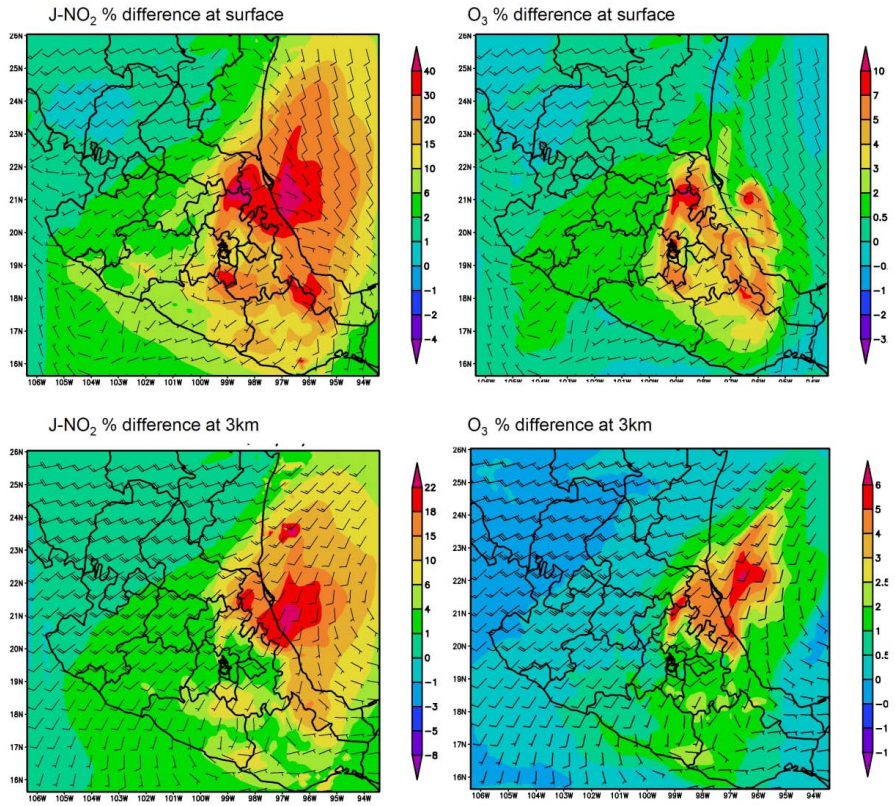

Fig. 7. Calculated modeled effect of aerosol loading on photolysis rate of NO_2 and O_3 formation calculated as difference between model runs with and without aerosol (NOOAD vs. base case) for 12 km STEM, 10 March 2006, at 21:00 UTC. Top panels calculated at surface layer; Bottom panels calculated at 3 km.

ACPD
8, 20283–20309, 2008

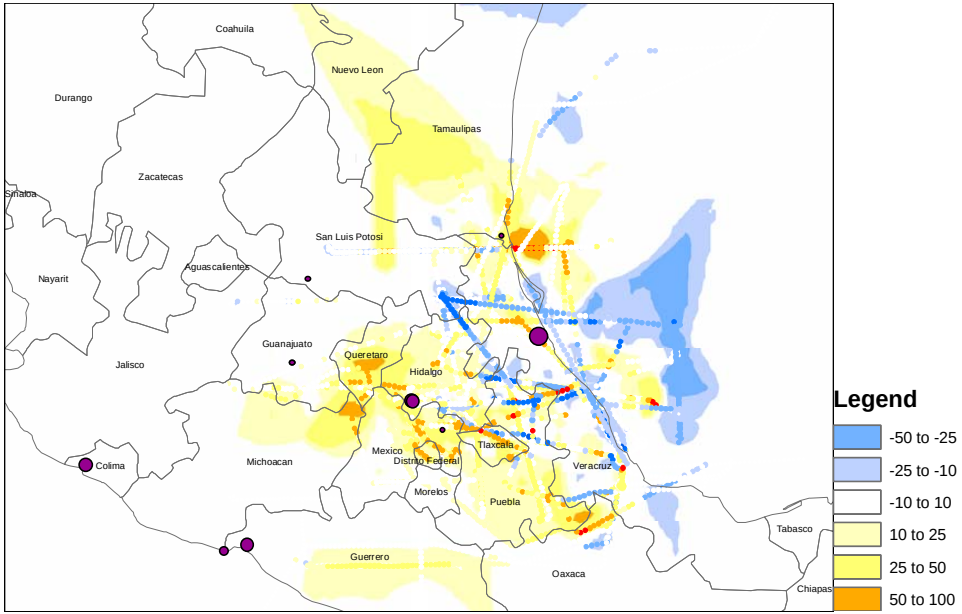

Fig. 8. Interpolated point percent bias of $J[NO_2 \rightarrow NO+O]$ modeling for values extracted along C-130 flight tracks using kriging, n=3500 for all science flights.

ACPD
8, 20283–20309, 2008